

See discussions, stats, and author profiles for this publication at: <https://www.researchgate.net/publication/229007582>

# Synthesis and Ultrafast Excited-State Dynamics of Zinc and Palladium Triply Fused Diporphyrins

ARTICLE in THE JOURNAL OF PHYSICAL CHEMISTRY A · JULY 2012

Impact Factor: 2.69 · DOI: 10.1021/jp3043895 · Source: PubMed

CITATIONS

5

READS

31

6 AUTHORS, INCLUDING:



**Derrick Andrew Roberts**

University of Cambridge

15 PUBLICATIONS 90 CITATIONS

SEE PROFILE



**Burkhard Fückel**

Max Planck Institute for Polymer Research

22 PUBLICATIONS 450 CITATIONS

SEE PROFILE



**Yuen Yap Cheng**

University of Sydney

30 PUBLICATIONS 619 CITATIONS

SEE PROFILE



**Timothy W Schmidt**

University of Sydney

119 PUBLICATIONS 1,463 CITATIONS

SEE PROFILE

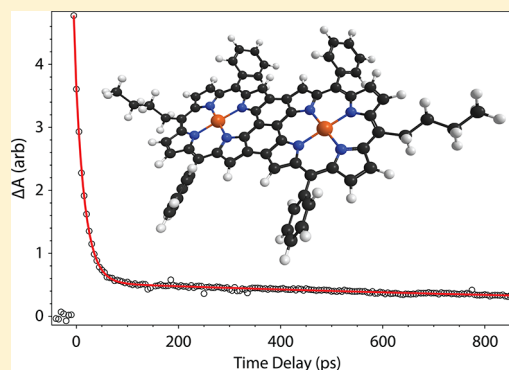
# Synthesis and Ultrafast Excited-State Dynamics of Zinc and Palladium Triply Fused Diporphyrins

Derrick A. Roberts, Burkhard Fückel, Raphaël G. C. R. Clady, Yuen Yap Cheng, Maxwell J. Crossley,\* and Timothy W. Schmidt\*

School of Chemistry, The University of Sydney, Sydney, NSW 2006, Australia

## S Supporting Information

**ABSTRACT:** We report the synthesis and ultrafast excited-state dynamics of two new meso–meso,  $\beta$ – $\beta$ ,  $\beta$ – $\beta$  triply fused diporphyrins, **Zn-3DP** and **Pd-3DP**. Both compounds were found to have short excited-state lifetimes: **Zn-3DP** possessed an average  $S_1$  lifetime of 14 ps before nonradiative deactivation to the ground state, whereas **Pd-3DP** displayed a longer average  $S_1$  lifetime of 18 ps before crossing to the  $T_1$  state, which itself possessed a very short triplet lifetime of 1.7 ns. The excited-state dynamics of **Zn-3DP**, compared to similar zinc(II) diporphyrins reported in the literature, suggests that a conical intersection of the  $S_1$  and  $S_0$  potential energy surfaces plays a major role as a deactivation pathway of these molecules. Furthermore, the short triplet lifetime of **Pd-3DP**, compared to other diporphyrins that also exploit the intramolecular heavy atom effect, reveals that the position of the heavy atom within the diporphyrin framework influences the strength of spin–orbit coupling. The implications for employing triply fused diporphyrins as NIR-absorbing triplet sensitizers are discussed.



## INTRODUCTION

Since their first reported synthesis over a decade ago,<sup>1</sup> meso–meso,  $\beta$ – $\beta$ ,  $\beta$ – $\beta$  triply fused porphyrin arrays have been the subject of intense research due to their extremely red-shifted absorption bands, high electrical conductivity, and nonlinear optical properties,<sup>1–5</sup> which render this class of molecule potentially useful for applications in molecular electronics,<sup>6</sup> reverse saturable absorption,<sup>7</sup> near-infrared sensing,<sup>8</sup> artificial photosynthesis,<sup>9</sup> and photodynamic therapy.<sup>10</sup> The latter applications are based on near-infrared (NIR) absorption features; hence, triply fused porphyrins can also be envisaged as NIR sensitizers for photochemical upconversion (PUC). In this process, two low-energy photons are fused incoherently to produce one photon of higher energy. Usually, PUC proceeds via sensitized triplet–triplet annihilation and thus makes use of metalloporphyrin sensitizers,<sup>11–13</sup> which possess large absorption cross sections and high intersystem crossing (ISC) rates. In previous work, we have employed a  $\pi$ -expanded tetrakisquinoxalinoporphyry, synthesized using a stepwise ring-annulation strategy,<sup>14,15</sup> as an efficient sensitizer for PUC of light in the 650–700 nm range.<sup>16,17</sup> Extending upconversion sensitization further into the NIR has been the focus of recent work in this field;<sup>13,18–20</sup> the wavelength regime above 900 nm, however, remains a barrier for PUC. The extremely red-shifted absorption bands of triply fused porphyrins have the potential to overcome this barrier.

While PUC mainly requires a high ISC yield and reasonably long triplet-state lifetime, the suitability of triply fused porphyrins for all of the applications listed above depends on

the dynamics of the involved excited electronic states. Organic molecules with electronic absorption bands in the NIR pose a particular challenge in this respect because the rate of excited-state deactivation typically increases exponentially as the electronic energy gaps decrease.<sup>21</sup> Therefore, it is crucial to understand the excited-state dynamics of triply fused porphyrins and their metal chelates in order to assess and tailor their photophysical properties for the aforementioned applications. The simplest representative of this class of molecule is the meso–meso,  $\beta$ – $\beta$ ,  $\beta$ – $\beta$  triply fused dimer (hereafter, triply fused diporphyrin), which serves as a useful model for understanding the excited-state dynamics of large aromatic heterocycles with extensive  $\pi$ -conjugation.

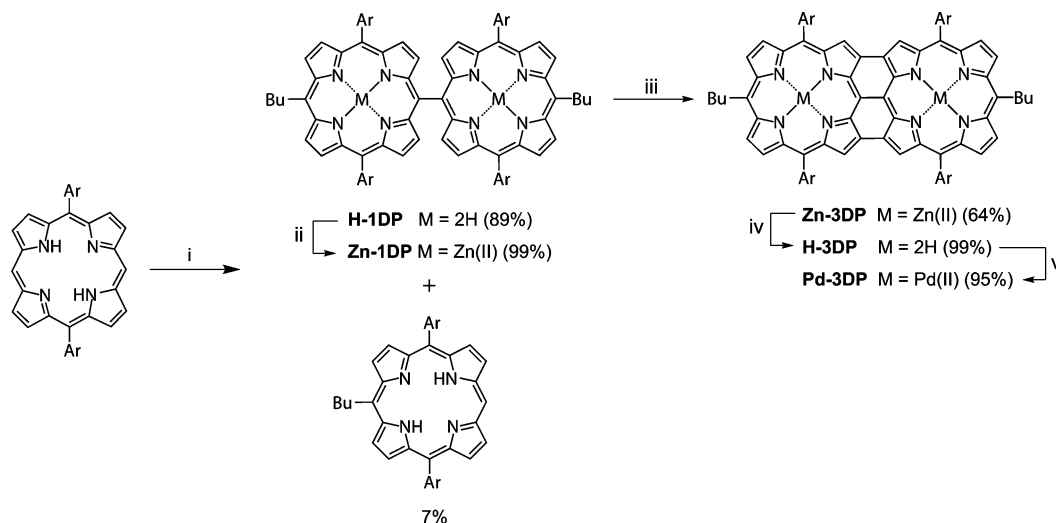
There are two key synthetic approaches to triply fused diporphyrins: (1) direct oxidative coupling of two monomeric porphyrins, each with at least one free meso position,<sup>22–26</sup> and (2) planarization of a meso–meso singly linked diporphyrin.<sup>1,3,9,27–30</sup> The first approach has become increasingly preferred in the recent literature; however, this method requires the use of 5,10,15-trisubstituted porphyrin precursors to prevent the formation of fused and linked oligomers, rather than dimers.<sup>6,31,32</sup> Unfortunately, the common routes to trisubstituted porphyrins are synthetically laborious when approached through the tripyrrane and inefficient via statistical condensation. The addition–dimerization methodology devel-

Received: May 7, 2012

Revised: July 5, 2012

Published: July 9, 2012



Scheme 1<sup>a</sup>

<sup>a</sup>Reagents and conditions: (i) *n*-butyllithium (1.4 M in hexanes),  $-78^\circ\text{C}$ , THF, 15 min and then DDQ, 30 min; (ii)  $\text{Zn(OAc)}_2 \cdot 2\text{H}_2\text{O}$  in  $\text{CHCl}_3$ – $\text{CH}_3\text{OH}$ , 1 h; (iii)  $\text{Sc(OTf)}_3$ –DDQ,  $50^\circ\text{C}$ , toluene, 1 h; (iv)  $\text{H}_2\text{SO}_4$ – $\text{CHCl}_3$ , rt, 5 min; (v)  $\text{Pd(OAc)}_2$  and NaOAc in  $\text{CHCl}_3$ – $\text{CH}_3\text{OH}$ , protected from light, 2 days. Ar = 3,5-di-*tert*-butylphenyl.

oped by Senge and co-workers addresses these shortcomings by offering a simple one-step route to end-capped meso–meso singly linked diporphyrins—the immediate precursors to triply fused diporphyrins.<sup>33,34</sup> The general methodology involves the reaction of a 5,15-disubstituted porphyrin with an alkyl or aryl organolithium reagent, followed by oxidative dimerization to afford a meso–meso singly linked diporphyrin.<sup>35</sup> The singly linked diporphyrin is readily converted to its triply fused counterpart by oxidative cyclodehydrogenation.<sup>1,4,22,26,30</sup>

While there has been sustained interest in developing synthetic methodologies toward triply fused diporphyrins, there has been comparatively little work on their excited-state dynamics. The research groups of Osuka, Kim, and Anderson have measured the excited-state dynamics of zinc(II) triply fused diporphyrins that differ only by their substitution at the meso-like positions around the diporphyrin core.<sup>2,7,23,36</sup> Interestingly, these structurally similar compounds display a wide range of excited-state behaviors, suggesting that the peripheral substituents have a pronounced influence on the dominant pathways through which excited-state deactivation occurs in these molecules. For instance, Osuka and co-workers reported an extremely short  $S_1$  lifetime (4.5 ps) and no triplet yield for a zinc(II) hexaaryl-substituted diporphyrin,<sup>36</sup> whereas Anderson and co-workers observed intersystem crossing and relatively long triplet lifetimes for zinc(II) diporphyrins whose terminal meso substituents had been replaced by iodo ( $\tau = 52$  ns), bromo ( $\tau = 280$  ns), and (triisopropylsilyl)alkynyl ( $\tau = 177$   $\mu\text{s}$ ) substituents.<sup>7</sup> Furthermore, there is ongoing debate regarding the dominant pathway of nonradiative  $S_1$  deactivation in triply fused diporphyrins. Therefore, further work on the excited-state dynamics of different triply fused diporphyrins is crucial for understanding their photophysical behavior for the aforementioned applications.

In this contribution we have synthesized zinc(II) and palladium(II) butyl-end-capped triply fused diporphyrins using a simple two-step synthetic route that combines the nucleophilic addition–dimerization methodology developed by Senge and co-workers<sup>33</sup> and the oxidative cyclodehydrogenation protocol reported by Osuka and co-workers,<sup>5</sup> which is

itself a variation of the Scholl reaction.<sup>37</sup> We subsequently measured the ultrafast excited-state dynamics of these diporphyrins in order to observe the effect of both *meso*-alkyl substitution and heavy metal chelation<sup>38</sup> on the  $S_1$  decay dynamics of these infrared chromophores. The excited-state dynamics of these two compounds are compared to diporphyrins reported in the recent literature and their photophysical properties are discussed in terms of applicability as sensitizers for PUC.

## ■ EXPERIMENTAL SECTION

**Organic Synthesis.** The synthesis details and characterization of the diporphyrins are described in the Supporting Information.

**Femtosecond Pump–Probe Laser Spectroscopy.** The dual-beam femtosecond time-resolved transient absorption setup consisted of a self-mode-locked femtosecond Ti-sapphire amplified fiber oscillator (Clark MXR, CPA 2210), two optical parametric amplifier systems (Light Conversion, TOPAS), and an optical detection system. The amplified output beam (780 nm) had  $\sim 150$  fs pulse width and a pulse energy of approximately 1.5 mJ at 1 kHz repetition rate, which was divided into two parts by a 1:1 beam splitter. Both beams were color-tuned to the desired pump and probe wavelengths by optical parametric amplification. The pump beam was directed through a variable delay stage and an optical chopper operating at 0.5 kHz and then focused to a  $\sim 2$  mm diameter spot on the sample cuvette, and the laser fluence was adjusted to avoid damage of the sample by using a variable neutral-density filter. The time delay between pump and probe beams was controlled by adjusting the length of the variable optical delay stage. Pump and probe beams were monitored after and before transmission through the sample by using high-speed photodiodes (ThorLabs and SM1 series, respectively) with home-built integration circuits. The difference between the signals with and without the pump beam were calculated by in-house software written in LabView.

## RESULTS AND DISCUSSION

**Diporphyrin Synthesis.** Synthesis of the target compounds is summarized in Scheme 1. Singly linked, butyl-end-capped diporphyrin **H-1DP** was synthesized in one step from readily available 5,15-bis(3,5-di-*tert*-butylphenyl)porphine using the nucleophilic addition–dimerization methodology developed by Senge and co-workers.<sup>33,35</sup> The reaction is understood to proceed through nucleophilic attack of *n*-butyllithium at a free porphyrin meso-position to give an anionic intermediate, which is then oxidized to its corresponding radical anion using DDQ (2,3-dichloro-5,6-dicyano-1,4-benzoquinone).<sup>35</sup> Homogenic bond formation at the remaining free meso carbon atoms and subsequent oxidation yields the singly linked product, **H-1DP**, which was obtained in 89% yield, with 7% of a monobutylated side product. As with other singly linked diporphyrins, **H-1DP** displays four unique  $\beta$ -pyrrolic resonances in its <sup>1</sup>H NMR spectrum (Supporting Information, Figure S1), characteristic of its C<sub>2</sub> symmetric structure, and a split Soret band in its electronic absorption spectrum due to excitonic coupling along the long axis of the dimer.

The formation of a monobutylated byproduct is attributed to protonation of the intermediate porphyrin anion, possibly as a result of intermolecular proton transfer between two intermediate porphyrin anions during the reaction. Senge and co-workers have demonstrated that 5,10,15-trisubstituted porphyrins are obtained as the major product of the reaction if water is added as a proton source before DDQ oxidation.<sup>33</sup> Accordingly, we found that extremely stringent control over the use of pure, anhydrous reagents was crucial to the success of this reaction. In particular, we found that using recrystallized and dried DDQ gave yields in excess of 85%, whereas using commercially purchased DDQ—thoroughly dried but without further purification—resulted in heavily suppressed reaction yields (23% of **H-1DP**) and an equal proportion of the monobutylated side product (24%).

These results demonstrate that the Senge methodology is a convenient and rapid route to meso–meso singly linked diporphyrins—a precursor to triply fused diporphyrins. The advantage of the Senge methodology over other routes to triply fused diporphyrins is that the terminal meso positions of the porphyrins are functionalized immediately prior to dimerization, thus preventing the uncontrolled formation of porphyrin oligomers that typically result from radical coupling methods, such as the Ag(I)-mediated coupling procedure reported by Aratani et al.<sup>39</sup> This approach therefore circumvents the need for 5,10,15-trisubstituted porphyrin starting materials. Furthermore, the end-capping groups of the diporphyrin can be modified depending on the choice of organolithium reagent, thus presenting the opportunity for installing further functionality after dimerization.

Diporphyrin **H-1DP** was metalated quantitatively to the zinc(II) chelate (**Zn-1DP**), which was planarized using Sc(OTf)<sub>3</sub>–DDQ as an oxidant to give the corresponding triply fused diporphyrin (**Zn-3DP**) in moderate yield (64%) (Scheme 1). Demetalation of **Zn-3DP** under acidic conditions afforded the free-base triply fused diporphyrin (**H-3DP**), which was smoothly converted to the palladium(II) chelate by treatment with Pd(OAc)<sub>2</sub> under basic conditions.

Electronic absorption spectra of **H-3DP**, **Zn-3DP**, and **Pd-3DP** are consistent with the spectra of hexaaryl-substituted diporphyrins,<sup>1,3,24</sup> displaying three distinct absorption bands (Figure 1). For consistency, these bands are labeled I, II, and III

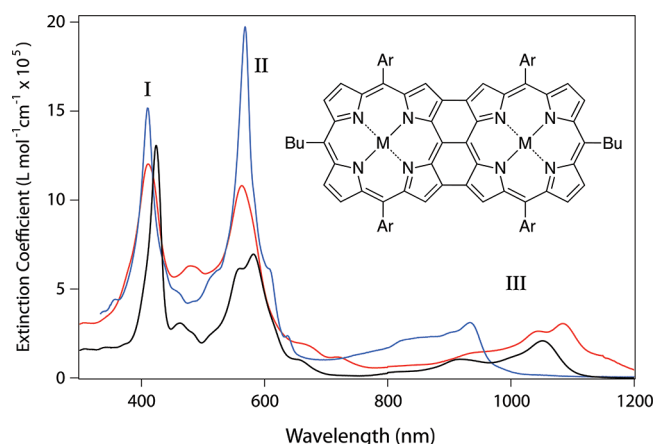


**Figure 1.** Electronic absorption spectra of **H-3DP** (red), **Zn-3DP** (black), and **Pd-3DP** (blue) in chloroform. Bands I, II, and III are consistent with reports by Osuka and co-workers.<sup>3</sup> Ar = 3,5-di-*tert*-butylphenyl.

according to the assignments by Osuka and co-workers: band I in the visible region, whose transition dipole moment is polarized along the short in-plane axis of the molecule, and bands II (visible) and III (NIR), whose transition dipole moments are both polarized along the long molecular axis.<sup>2,3</sup>

The purity of the triply fused diporphyrins was confirmed by high-resolution LDI-FTICR mass spectrometry, UV–vis–NIR spectroscopy, and <sup>1</sup>H NMR analysis where possible (see Supporting Information, Figure S3–S7). Both **Zn-3DP** and **Pd-3DP** displayed broad <sup>1</sup>H NMR signals in deuterated chloroform, suggesting that the molecules aggregate in solution at the concentrations required for obtaining readable NMR spectra. Adding a small amount of pyridine-*d*<sub>5</sub> to the sample in CDCl<sub>3</sub> improved the quality of the <sup>1</sup>H NMR spectrum of **Zn-3DP** but did not noticeably ameliorate aggregation of **Pd-3DP**.

Recently, Senge et al. reported an attempt to combine the addition–dimerization coupling methodology with the Sc(OTf)<sub>3</sub>–DDQ cyclodehydrogenation reaction employed by Osuka and co-workers as a route to a hexasubstituted triply fused porphyrin dimer.<sup>40</sup> In this work, the authors reported that the reaction of a zinc(II) hexyl-end-capped singly linked diporphyrin with up to 7 equiv of Sc(OTf)<sub>3</sub>–DDQ failed to afford any triply fused product. This result is in stark contrast to our own experience with **Zn-1DP**, which was converted to its triply fused counterpart under similar conditions. We did, however, find that oxidative cyclodehydrogenation could not be performed with **H-1DP**, which can be explained by the fact that the first and second oxidation potentials of **H-1DP** are significantly higher than those of **Zn-1DP**.<sup>3</sup>

**Excited-State Dynamics.** The excited-state dynamics of **Zn-3DP** and **Pd-3DP** were measured by ultrafast transient absorption spectroscopy using a femtosecond pump–probe pulsed laser experimental setup. Both diporphyrins were found to have very short excited-state lifetimes, which is consistent with previous work on other triply fused diporphyrins.<sup>2,7,23,36</sup>

**Zinc(II) Triply Fused Diporphyrin (Zn-3DP).** Ultrafast excited-state absorption transients on **Zn-3DP** are shown in Figure 2. In both cases, a deoxygenated chloroform solution of the diporphyrin ( $5.7 \times 10^{-5}$  M) was excited at a pump wavelength of 1090 nm, exciting at the peak of band III to prepare vibrationally excited molecules in their S<sub>1</sub> electronic state. The solutions were then probed at 580 and 700 nm to monitor recovery of the ground state difference signal.



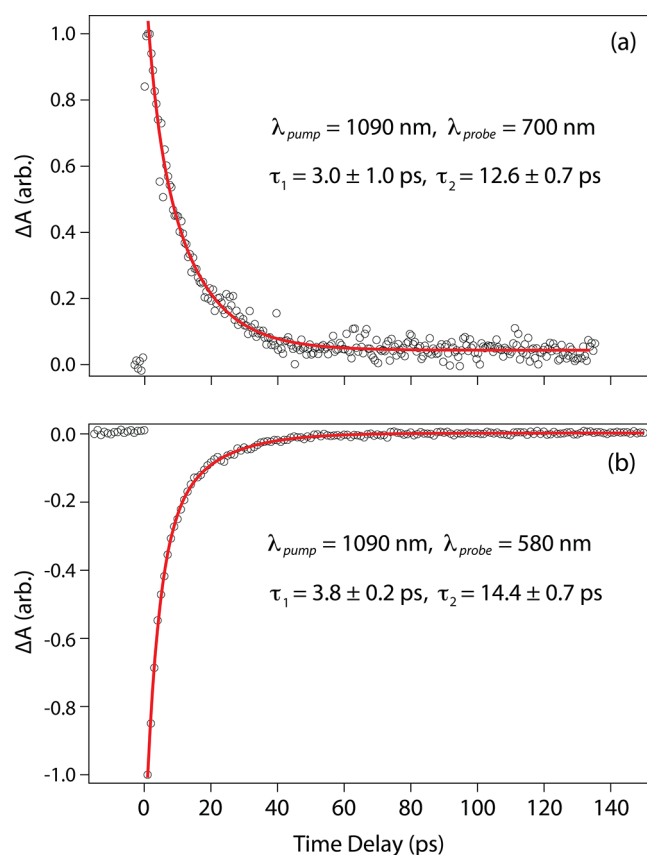


**Figure 2.** Ultrafast transient absorption dynamics of **Zn-3DP** in chloroform, pumping at 1090 nm and probing at (a) 700 nm and (b) 580 nm. The experimental data are fitted to a biexponential decay model (solid red line).

At a probe wavelength of 580 nm, the transient absorption consisted of ground state bleaching followed by complete biexponential recovery to the prepump difference signal ( $\Delta A = 0$ ), with decay constants of  $3.8 \pm 0.2$  and  $14.4 \pm 0.7$  ps contributing to 57 and 43% of the total decay profile, respectively. Excited-state absorption was observed at the 700 nm probe wavelength, followed by near-complete biexponential recovery to the prepump difference signal with decay constants of  $3.0 \pm 1.0$  and  $12.6 \pm 0.7$  ps, contributing to 23 and 77% of the observed decay profile, respectively. Close observation of the decay profile at  $\lambda_{pr} = 700$  nm reveals incomplete recovery of the difference signal, thus suggesting that **Zn-3DP** might possess a very small triplet yield.

Cho et al. have also reported biexponential decay processes in an hexaaryl triply fused zinc(II) diporphyrin, whereby a short decay component (4.5 ps) was attributed to extremely rapid  $S_1 \rightarrow S_0$  deactivation, and a much longer component (2.2 ns) was tentatively assigned to the excited-state dynamics of a monomeric porphyrin contaminant in the experimental sample.<sup>2</sup> The relative contributions of the fast and slow decay components were 98 and 2%, respectively. These authors also recorded fluorescence from the  $S_2$  state with a lifetime of 15 ps and a very small fluorescence quantum yield of  $\sim 10^{-5}$ , suggesting that either their diporphyrin disobeys Kasha's rule or that the putative contaminant in their sample gave rise to the observed fluorescence. These findings differ substantially from our own, not only in the decay components but, moreover, we did not observe fluorescence in the 600–700 nm range upon excitation of the Soret band that could be attributed to **Zn-**

**3DP**. In our experiment, molecules in the sample are excited only to  $S_1$  using a pump wavelength of 1090 nm; as such, deactivation processes from within the  $S_1$  manifold are observable. Therefore, we assign the fast (3 ps) decay component to nonradiative relaxation from an excited vibrational level within the  $S_1$  state followed by rapid  $S_1 \rightarrow S_0$  (and some  $S_1 \rightarrow T_1$ ) deactivation (14 ps), most likely dominated by nonradiative processes based on the very short lifetime of the  $S_1$  state (Figure 3a). These decay constants are consistent with the 10–20 ps time scales observed for nonradiative decay in other multiporphyrin arrays.<sup>41,42</sup>

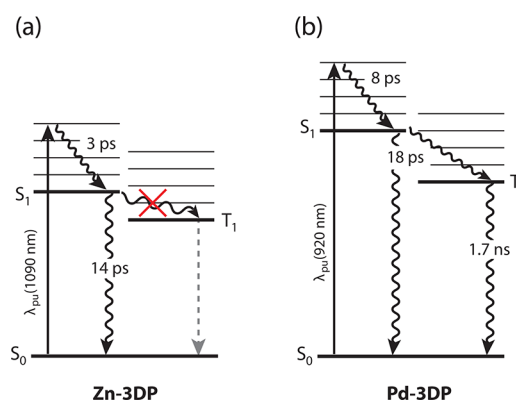


**Figure 3.** Jablonski diagrams summarizing the ultrafast excited-state dynamics of metalldiporphyrins (a) **Zn-3DP** and (b) **Pd-3DP**.

The reason for the different excited state dynamics we observed for **Zn-3DP**, compared with the results of Cho et al.,<sup>43</sup> are not clear but appear to be strongly influenced by substituent effects around the diporphyrin core. Indeed, reports of other zinc(II) triply fused diporphyrins, differing only by their peripheral substituents, display vastly different excited-state behaviors.<sup>7,23,43</sup> This point will be discussed in further detail in the following sections.

**Palladium(II) Triply Fused Diporphyrin (Pd-3DP).** Transient absorption dynamics at various probe wavelengths are displayed in Figure S6 (Supporting Information). The resulting transient absorption spectra from the  $S_1$  and  $T_1$  states are depicted in Figure 4 with the decay lifetimes summarized in Figure 5.

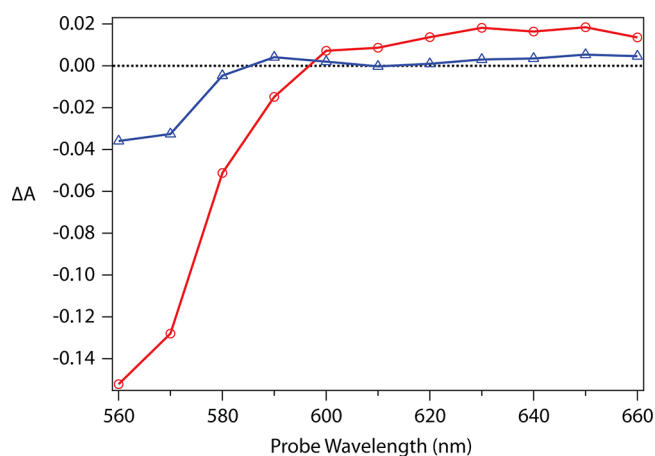


**Figure 4.** Transient absorption spectra of the  $S_1$  (red circles) and  $T_1$  (blue triangles) states of **Pd-3DP**. Pump wavelength was fixed at 920 nm.

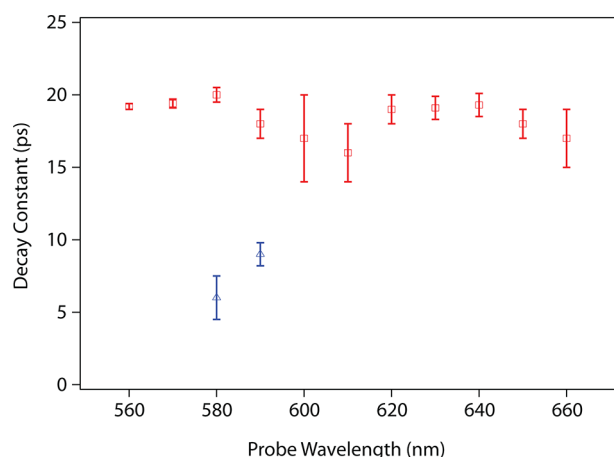


**Figure 5.** Summary of the excited state lifetimes of **Pd-3DP** at various probe wavelengths between 560 and 660 nm. All traces were fitted to a monoexponential decay function, except for  $\lambda_{\text{probe}}$  at 580 and 590 nm, which exhibited biexponential decay dynamics. Slow decay components are shown in red; fast decay components are shown in blue. Error bars indicate one standard deviation in the curve-fitting procedure.

A chloroform solution of **Pd-3DP** ( $2.4 \times 10^{-5}$  M) was excited at a pump wavelength of 920 nm, exciting at the peak of band III, to prepare molecules in their  $S_1$  electronic states. The sample was then probed at 10 nm intervals from 560 to 660 nm, and the time-resolved transient absorption profiles were recorded (Supporting Information, Figure S6). Ground-state bleaching was observed for probe wavelengths at and below 590 nm, and excited-state absorption was observed at wavelengths above 600 nm. In each case, the difference signal did not recover to the prepump level but instead displayed a persistent nonzero difference signal that decayed with a time constant of 1.7 ns (Figure 6). Since the pump beam was selected to excite the absorbing molecules to  $S_1$ , the most likely state that could give rise to a persistent nonzero difference signal is  $T_1$ . As such, we propose that **Pd-3DP** crosses to the  $T_1$  state following photoexcitation to  $S_1$ , followed by rapid nonradiative decay back to the ground state. This observation is consistent with the

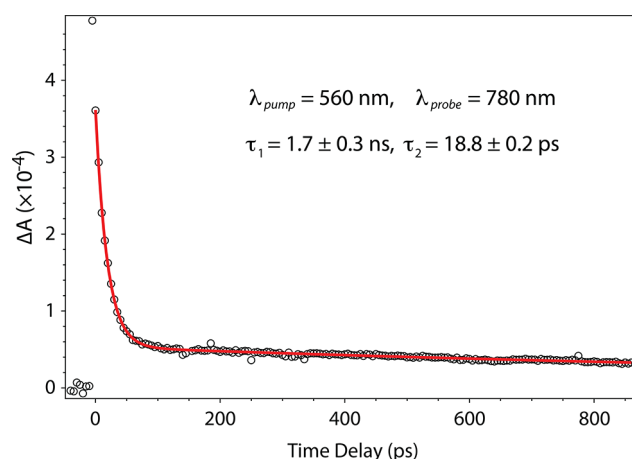


**Figure 6.** Ultrafast transient absorption dynamics of **Pd-3DP** in chloroform using an extended time delay, pumping at 560 nm, and probing at 780 nm. Experimental data are fitted to a biexponential decay model (red line).

heavy atom effect due to the larger atomic mass of palladium compared to zinc.<sup>38</sup>

The  $T_1$  lifetime of **Pd-3DP** was measured using pump and probe wavelengths of 560 and 780 nm, respectively, and extending the pump–probe time delay to 900 ps (the maximum delay on our instrumentation). The resulting ground state bleach and biexponential recovery revealed a very short  $T_1$  lifetime of  $1.7 \pm 0.3$  ns, which we attribute to strong  $T_1 \rightarrow S_0$  reverse ISC due both to spin–orbit coupling introduced by the heavy palladium nucleus and the relatively small  $T_1$ – $S_0$  energy gap expected for this molecule. This observation represents a manifestation of the heavy atom effect that is highly undesirable for applications such as photodynamic therapy and PUC, which require molecules with long-lived triplet states. A similar result was reported by Anderson and co-workers, who observed no triplet yield on the nanosecond time scale for a lead(II) triply fused diporphyrin.<sup>7</sup> Interestingly, the authors did note a significant triplet yield and lifetime on the order of 250 ns for a meso-brominated zinc(II) triply fused diporphyrin.<sup>7</sup> These results underscore the care with which the heavy atom effect should be employed when trying to synthesize compounds with high triplet yields and lifetimes, especially since the heavy atom effect is only one of many factors that govern intersystem crossing efficiency and triplet lifetime in organic molecules.<sup>38</sup>

The  $S_1$  decay profile at each probe wavelength was fitted to a monoexponential decay function, with the exception of the experiments probing at 580 and 590 nm, which were better described by a biexponential model (Supporting Information, Figure S6). These experiments returned an average long decay component with a time constant of  $18.0 \pm 1.0$  ps and a shorter decay component with a time constant of  $8.0 \pm 1.0$  ps (Figure 5). The suitability of the biexponential fits at 580 and 590 nm probe wavelengths suggests that the probe beam is illuminating two concomitant deactivation processes. We ascribe the fast decay process (8 ps) to vibrational cooling within the  $S_1$  manifold, while the slower decay process (18 ps) is assigned to deactivation of  $S_1$  via both singlet and triplet channels (Figure 3).

The dynamics can be modeled in terms of three states with differing absorption properties. Molecules are initially prepared in  $S_1^*$ , which relaxes at rate  $k_1$  to  $S_1$ . This vibrationally relaxed, electronically excited level then decays back to  $S_0$  (and  $T_1$ ) at rate  $k_2$ . Thus

$$[S_1^*]_t = [S_1^*]_0 \exp(-k_1 t) \quad (1)$$

$$[S_1]_t = \frac{[S_1^*]_0 k_1}{k_1 - k_2} (\exp(-k_2 t) - \exp(-k_1 t)) \quad (2)$$

and

$$[S_0]_t + [T_1]_t = [S_1^*]_0 \left( \frac{k_2 \exp(-k_1 t)}{k_1 - k_2} - \frac{k_1 \exp(-k_2 t)}{k_1 - k_2} + 1 \right) \quad (3)$$

The transient absorption signal may be modeled as the sum of the contributions from the three species

$$\Delta A_t(\lambda) = l \sum_i^3 \Delta \epsilon_i(\lambda) [i]_t \quad (4)$$

where  $l$  is the path length, and  $\Delta\epsilon_i(\lambda)$  is the difference of the extinction coefficients of species  $i$  and the unexcited chromophore at wavelength  $\lambda$ . The quantity  $\Delta A_i(\lambda)$  may thus be fit to a constant and two exponential terms.

Intuitively, both the fast and the slow decay processes should be occurring at each probe wavelength. However, they are only observable at probe wavelengths of 580 and 590 nm. This can be explained by considering the transient absorption spectra for a vibrationally excited sublevel and the vibrational ground state of  $S_1$ , as depicted schematically in Figure 7. Upon initial

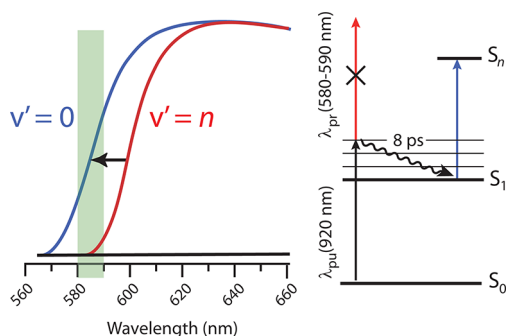


**Figure 7.** Schematic depicting the positions of the transient absorption spectra in a vibrationally excited state (red) and at the vibrationless level (blue) of  $S_1$ , which would give rise to the excited state dynamics observed for **Pd-3DP**. Nonradiative decay of the hot-band spectrum would be most clearly noticed in the shaded region.

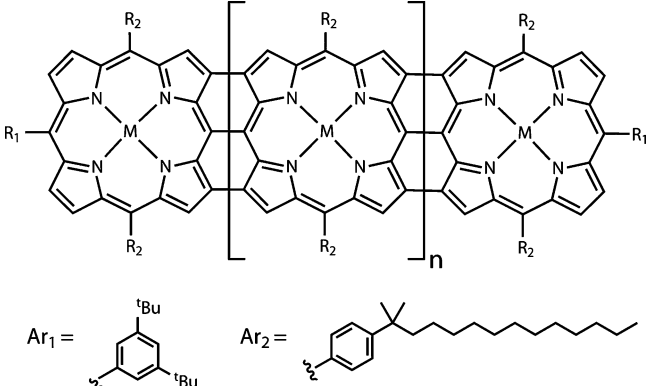
excitation, the transient absorption is dominated by hot band transitions from  $S_1$  (red spectrum). As nonradiative decay to the vibrationless level in  $S_1$  occurs, the transient absorption spectrum shifts to shorter wavelengths (blue spectrum). The edge of the hot band spectrum is between 590 and 600 nm, which can be inferred from the change from bleaching to

induced absorption between these two probe wavelengths (Figure 4). Therefore, after blue-shifting due to vibrational relaxation within  $S_1$ , the molecule absorbs more strongly at 580 and 590 nm. As a result, the vibrational cooling processes within  $S_1$ —on the order of 8 ps—are observable at these probe wavelengths, manifesting in an apparent increase in the rate of recovery of the ground-state difference signal. The reason as to why this behavior was not observed at other wavelengths is that the change in signal intensity upon vibrational cooling is only significant at the band edge, particularly as the diporphyrin excited-state absorption bands are quite sharp in the region 570–590 nm (cf. Figure 4). This behavior is reminiscent of the ultrafast transient absorption dynamics of sterically crowded nickel(II) porphyrins reported by Holten and co-workers, who observed wavelength-dependent vibrational relaxation on the order of 7 ps within the excited state manifolds of these porphyrins.<sup>45,46</sup>

The longer  $S_1$  lifetime of **Pd-3DP** compared with **Zn-3DP** can be explained by the larger  $S_1$ – $S_0$  energy gap in the former compound. This is evident from the blue-shifting of band III in the electronic absorption spectrum of **Pd-3DP** (Figure 1), with respect to **Zn-3DP**, which suggests that palladium(II) has a similar effect on stabilizing the HOMO ( $b_{2g}$ )<sup>44</sup> of the diporphyrin as it does with the  $a_{2u}$  orbital in monomeric porphyrins.

**Trends in Excited-State Dynamics of Diporphyrins.** Comparing the excited-state lifetimes of **Zn-3DP** and **Pd-3DP** with similar triply fused diporphyrins reported in the literature provides further insight into the photophysical trends within this class of molecule. The groups of Osuka, Kim, and Anderson have measured the excited-state dynamics of other triply fused diporphyrins, which exhibit vastly different behavior despite very similar molecular structures (cf. Table 1).<sup>2,7,23,36</sup> On the basis of the data compiled in Table 1, the substituents

**Table 1.** Comparison of the Excited State Dynamics of Triply Fused Metallodiporphyrins<sup>a</sup>

									
	$n$	$R_1$	$R_2$	M	$\tau(S_1)$	$\tau(T_1)$	$\Phi(T_1)$	solvent	reference
1	1	Ar <sub>1</sub>	Ar <sub>2</sub>	Zn(II)	2.3 ± 0.2 ps	—	—	toluene	2
2	0	Ar <sub>1</sub>	Ar <sub>2</sub>	Zn(II)	4.5 ± 0.5 ps	—	—	toluene	2
<b>Zn-3DP</b>	0	Bu	Ar <sub>1</sub>	Zn(II)	13.5 ± 0.7 ps	—	<sup>a</sup>	CHCl <sub>3</sub>	herein
3	0	Br/I	Ar <sub>1</sub>	Pb(II)	<5 ns	—	—	CHCl <sub>3</sub> /pyridine	7
<b>Pd-3DP</b>	0	Bu	Ar <sub>1</sub>	Pd(II)	18.0 ± 1.0 ps	1.7 ± 0.3 ns	—	CHCl <sub>3</sub>	herein
4	0	I	Ar <sub>1</sub>	Zn(II)	—	52 ns	0.2	CHCl <sub>3</sub> /pyridine	7
5	0	Br	Ar <sub>1</sub>	Zn(II)	—	280 ns	0.12	CHCl <sub>3</sub> /pyridine	7
6	0	C≡C–Si( <sup>t</sup> Pr) <sub>3</sub>	Ar <sub>1</sub>	Zn(II)	—	177 ± 25 μs	<sup>b</sup>	CHCl <sub>3</sub> /pyridine	23

<sup>a</sup>For compounds 3–6, the solvent is 1% (v/v) pyridine in CHCl<sub>3</sub>. Specific excited-state values were not reported for dashed entries. <sup>b</sup>Triplet yields for these molecules were extremely small.

around the periphery of the diporphyrin core appear to influence the excited-state dynamics of the molecule strongly. For instance, excited-state deactivation is extremely rapid (<5 ps) in porphyrin tapes with only aryl substituents (**1** and **2**), and the decay constant of deactivation is the same regardless of the pump wavelength.<sup>2</sup> Changing the substituents at the terminal meso-like positions to (triisopropylsilyl)alkynyl (**4**), bromo (**5**), or iodo (**6**) groups results in diporphyrins with measurable triplet yields and triplet lifetimes ranging from tens of nanoseconds to hundreds of microseconds.<sup>7,23</sup>

The dominant pathway of nonradiative deactivation in triply fused diporphyrins remains under debate. Osuka and colleagues have attributed the ultrafast  $S_1$  decay of compounds **1**, **2**, and related porphyrin tapes ( $n > 1$ ), which have  $S_1$  lifetimes on the order of 2–5 ps, to internal conversion as described by the energy gap law.<sup>2,36</sup> Anderson and co-workers have recently reported, however, that extensive deuteration of the triply fused diporphyrin framework has no effect on the fluorescence quantum yield of the molecule.<sup>23</sup> Since C–H vibrations strongly influence the Franck–Condon factor of internal conversion, this finding indicates that nonradiative deactivation of the diporphyrin  $S_1$  state is not governed by  $S_1$ – $S_0$  internal conversion. Instead, Anderson and co-workers propose an alternative deactivation pathway involving a conical intersection of the  $S_1$  and  $S_0$  potential energy surfaces.<sup>23</sup>

Comparing the excited state dynamics of **Zn-3DP** with diporphyrin **2** provides an interesting insight to this ongoing debate. Both compounds have identical ground-state electronic absorption spectra, signifying that the positions of their electronic energy levels are very similar. However, the  $S_1$  lifetime of **Zn-3DP** is more than three times that of **2** and nearly seven times shorter than the ~100 ps  $S_1$  lifetime that Frampton et al. calculated for nonradiative deactivation according to the energy gap law (based on an  $S_1$ – $S_0$  energy gap of 109 kJ mol<sup>−1</sup> or 1100 nm).<sup>23</sup> Therefore, it follows that the energy gap law alone is not sufficient to explain the rate of  $S_1$ → $S_0$  deactivation in these triply fused diporphyrins. On the basis of this apparent substituent effect, it seems likely that the meso substituents strongly affect the access to the conical intersection as put forward by Anderson and co-workers.<sup>23</sup> Hence, while it is undoubtedly true that the  $S_1$ – $S_0$  energy gap generally influences the rate of nonradiative decay in organic molecules, the excited-state dynamics of **Zn-3DP** and **2** suggest that there is not a simple relationship between the  $S_1$ – $S_0$  energy gap and nonradiative deactivation rates in triply fused diporphyrins.

Rapid nonradiative deactivation of the  $S_1$  state in diporphyrins **1**, **2**, and **Zn-3DP**, and their negligible triplet yields, severely limits their suitability for many photophysical and photochemical applications—in particular as sensitizer compounds for PUC. A common approach for increasing the triplet yield of an organic compound is to incorporate heavy atoms into its molecular structure.<sup>38</sup> The heavy atom introduces electronic spin–orbit coupling, thus accelerating the rate of ISC. The success of this concept can be seen by the increased triplet yields of heavy atom-containing diporphyrins **Pd-3DP**, **4**, and **5** as compared to diporphyrins **1**, **2**, and **Zn-3DP** (Table 1). The heavy atom effect also has the adverse consequence of drastically decreasing the triplet lifetime due to the increased rate of  $T_1$ → $S_0$  reverse ISC. Notably, the triplet lifetimes decrease in the order of  $\tau_5 > \tau_4 > \tau_3$  as the atomic number of the corresponding heavy atom increases  $Z_{\text{Br}} < Z_{\text{I}} < Z_{\text{Pb}}$ . The fact that **Pd-3DP** has a shorter triplet lifetime than **4**,

despite palladium having a lower atomic number than iodine, suggests that the position of the heavy atom within the diporphyrin framework influences the degree to which spin–orbit coupling is affected. A possible reason for this observation could originate from the large spin density on the pyrrolic nitrogen atoms predicted for the HOMO and LUMO orbitals of the triply fused diporphyrin,<sup>44</sup> thus resulting in a strong interaction between the metal center and the  $\pi$ -electrons of the porphyrin excited state. In terms of its applicability for PUC, the short triplet lifetime of **Pd-3DP** precludes its use as a sensitizer molecule. Indeed, an emitter concentration of ~1 M would be needed for sufficient triplet energy transfer.

Zinc(II) diporphyrin **6**, with (triisopropylsilyl)alkynyl terminal meso substituents, has a very long triplet lifetime (177  $\mu$ s) compared to the other diporphyrins in Table 1. However, Anderson and co-workers found that the triplet yield of this compound is extremely low,<sup>7</sup> which is consistent with the absence of a heavy nucleus from the molecular structure and also with the low triplet yields typically observed in zinc(II) porphyrins.<sup>38</sup> Hence, the rate of ISC in **6** is slow, which results in both a low triplet yield (slow  $S_1$ → $T_1$ ) and a long triplet lifetime (slow  $T_1$ → $S_0$ ). Although the triplet state of **6** is sufficiently long-lived for undergoing energy transfer, the very low triplet yield limits its utility for PUC. On the basis of the data in Table 1, incorporation of heavy atoms around the periphery of the diporphyrin, as exemplified by meso-brominated diporphyrin **5**, represents the most promising concept for achieving an acceptable balance between triplet yield and lifetime.

## CONCLUSIONS

We have synthesized butyl-end-capped triply fused diporphyrins **Zn-3DP** and **Pd-3DP** in good yields using an efficient two-step strategy that combines the work of the Senge and Osuka research groups.<sup>5,33</sup> The ultrafast excited-state dynamics of these diporphyrins were subsequently measured and compared with similar compounds in the recent literature, revealing that the substituents in the terminal (15,15') meso positions of the diporphyrin strongly influence the excited-state dynamics of the molecule. Different excited-state dynamics observed for **Zn-3DP** and literature<sup>2</sup> diporphyrin **2**, despite similar chemical structures and identical electronic absorption spectra, suggests that the energy gap law alone does not explain the rapid excited-state deactivation observed for these molecules. The hypothesis of nonradiative deactivation via a crossing of the  $S_1$ – $S_0$  potential energy surfaces, as proposed by Anderson and co-workers,<sup>23</sup> is consistent with our data.

Triply fused diporphyrins are potential candidates for application as NIR sensitizer materials in PUC due to their intense NIR absorption features. While the compounds reported herein lack the triplet yield and lifetime for immediate application, comparison with different diporphyrins reveals trends for improvement. Notably, metalation of the diporphyrin with palladium(II) has the consequence of increasing  $T_1$ → $S_0$  reverse ISC significantly, thus resulting in a very short triplet lifetime. However, replacing meso-substituents with halogen (Br, I) atoms produces a reasonable balance between triplet yield and triplet lifetime, also indicating that the position of the heavy atom within the diporphyrin framework influences how the heavy atom effect manifests. Hence, modifications at the periphery of the diporphyrin framework seem to offer the most promising route to NIR-PUC sensitizers.



## ■ ASSOCIATED CONTENT

## ■ Supporting Information

Full synthetic details and characterization of the diporphyrins, selected  $^1\text{H}$  NMR and mass spectra and time-resolved transient absorption dynamics traces for Pd-3DP. This material is available free of charge via the Internet at <http://pubs.acs.org>.

## ■ AUTHOR INFORMATION

## Corresponding Author

\*E-mail: [maxwell.crossley@sydney.edu.au](mailto:maxwell.crossley@sydney.edu.au) (M.J.C.), [timothy.schmidt@sydney.edu.au](mailto:timothy.schmidt@sydney.edu.au) (T.W.S.).

## Notes

The authors declare no competing financial interest.

## ■ ACKNOWLEDGMENTS

D.A.R. acknowledges the Australian government for an Australian Postgraduate Award and the University of Sydney for an Honours Scholarship and the Vice Chancellor's Research Scholarship. D.A.R. thanks Prof. Jeffrey Reimers for helpful discussions. B.F. acknowledges the Alexander von Humboldt-Foundation for a Feodor Lynen fellowship. R.G.C.R.C. acknowledges the Australian Solar Institute for a postdoctoral research fellowship. Y.C. acknowledges The University of Sydney for a Gritton Fellowship. The authors thank Duncan Wild for assistance with building the integrating photodiodes. This research project is funded by the Australian Solar Institute, with contributions from The New South Wales Government and The University of Sydney. Aspects of this research were supported under Australian Research Councils Discovery Projects funding scheme (DP110103300 to T.W.S. and DP1092560 to M.J.C.). Equipment was purchased with support from the Australian Research Council (LE0668257).

## ■ REFERENCES

- (1) Tsuda, A.; Furuta, H.; Osuka, A. *Angew. Chem., Int. Ed.* **2000**, *39*, 2549–2552.
- (2) Cho, H. S.; Jeong, D. H.; Cho, S.; Kim, D.; Matsuzaki, Y.; Tanaka, K.; Tsuda, A.; Osuka, A. *J. Am. Chem. Soc.* **2002**, *124*, 14642–14654.
- (3) Tsuda, A.; Furuta, H.; Osuka, A. *J. Am. Chem. Soc.* **2001**, *123*, 10304–10321.
- (4) Tsuda, A.; Osuka, A. *J. Inclusion Phenom. Macrocycl. Chem.* **2001**, *41*, 77–81.
- (5) Tsuda, A.; Osuka, A. *Science* **2001**, *293*, 79–82.
- (6) Ikeda, T.; Aratani, N.; Osuka, A. *Chem.-Asian J.* **2009**, *4*, 1248–1256.
- (7) McEwan, K. J.; Fleitz, P. A.; Rogers, J. E.; Slagle, J. E.; McLean, D. G.; Akdas, H.; Katterle, M.; Blake, I. M.; Anderson, H. L. *Adv. Mater.* **2004**, *16*, 1933–1935.
- (8) Diev, V. V.; Hanson, K.; Zimmerman, J. D.; Forrest, S. R.; Thompson, M. E. *Angew. Chem., Int. Ed.* **2010**, *49*, 5523–5526.
- (9) Bonifazi, D.; Accorsi, G.; Armaroli, N.; Song, F. Y.; Palkar, A.; Echegoyen, L.; Scholl, M.; Seiler, P.; Jaun, B.; Diederich, F. *Helv. Chim. Acta* **2005**, *88*, 1839–1884.
- (10) Dougherty, T. J.; Gomer, C. J.; Henderson, B. W.; Jori, G.; Kessel, D.; Korbek, M.; Moan, J.; Peng, Q. *J. Natl. Cancer Inst.* **1998**, *90*, 889–905.
- (11) Singh-Rachford, T. N.; Castellano, F. N. *Coord. Chem. Rev.* **2010**, *254*, 2560–2573.
- (12) Zhao, J. Z.; Ji, S. M.; Guo, H. M. *RSC Adv.* **2011**, *1*, 937–950.
- (13) Yakutkin, V.; Aleshchenkov, S.; Chernov, S.; Miteva, T.; Nelles, G.; Cheprakov, A.; Balushev, S. *Chem.-Eur. J.* **2008**, *14*, 9846–9850.
- (14) Crossley, M. J.; Sheehan, C. S.; Khoury, T.; Reimers, J. R.; Santic, P. *J. New J. Chem.* **2008**, *32*, 340–352.
- (15) Khoury, T.; Crossley, M. J. *Chem. Commun.* **2007**, 4851–4853.
- (16) Cheng, Y. Y.; Khoury, T.; Clady, R.; Tayebjee, M. J. Y.; Ekins-Daukes, N. J.; Crossley, M. J.; Schmidt, T. W. *Phys. Chem. Chem. Phys.* **2010**, *12*, 66–71.
- (17) Cheng, Y. Y.; Fückel, B.; Khoury, T.; Clady, R. G. C. R.; Tayebjee, M. J. Y.; Ekins-Daukes, N. J.; Crossley, M. J.; Schmidt, T. W. *J. Phys. Chem. Lett.* **2010**, *1*, 1795–1799.
- (18) Balushev, S.; Yakutkin, V.; Miteva, T.; Avlasevich, Y.; Chernov, S.; Aleshchenkov, S.; Nelles, G.; Cheprakov, A.; Yasuda, A.; Mullen, K.; Wegner, G. *Angew. Chem., Int. Ed.* **2007**, *46*, 7693–7696.
- (19) Fückel, B.; Roberts, D. A.; Cheng, Y. Y.; Clady, R.; Piper, R. B.; Ekins-Daukes, N. J.; Crossley, M. J.; Schmidt, T. W. *J. Phys. Chem. Lett.* **2011**, *2*, 966–971.
- (20) Singh-Rachford, T. N.; Nayak, A.; Muro-Small, M. L.; Goeb, S.; Therien, M. J.; Castellano, F. N. *J. Am. Chem. Soc.* **2010**, *132*, 14203–11.
- (21) Englman, R.; Jortner, J. *Mol. Phys.* **1970**, *18*, 145–164.
- (22) Brennan, B. J.; Kenney, M. J.; Liddell, P. A.; Cherry, B. R.; Li, J.; Moore, A. L.; Moore, T. A.; Gust, D. *Chem. Commun.* **2011**, *47*, 10034–10036.
- (23) Frampton, M. J.; Accorsi, G.; Armaroli, N.; Rogers, J. E.; Fleitz, P. A.; McEwan, K. J.; Anderson, H. L. *Org. Biomol. Chem.* **2007**, *5*, 1056–1061.
- (24) Kamo, M.; Tsuda, A.; Nakamura, Y.; Aratani, N.; Furukawa, K.; Kato, T.; Osuka, A. *Org. Lett.* **2003**, *5*, 2079–2082.
- (25) Nakamura, Y.; Aratani, N.; Tsuda, A.; Osuka, A.; Furukawa, K.; Kato, T. *J. Porphyrins Phthalocyanines* **2003**, *7*, 264–269.
- (26) Ouyang, Q.; Zhu, Y. Z.; Zhang, C. H.; Yan, K. Q.; Li, Y. C.; Zheng, J. Y. *Org. Lett.* **2009**, *11*, 5266–5269.
- (27) Blake, I. M.; Krivokapic, A.; Katterle, M.; Anderson, H. L. *Chem. Commun.* **2002**, 1662–1663.
- (28) Bonifazi, D.; Scholl, M.; Song, F. Y.; Echegoyen, L.; Accorsi, G.; Armaroli, N.; Diederich, F. *Angew. Chem., Int. Ed.* **2003**, *42*, 4966–4970.
- (29) Inokuma, Y.; Ono, N.; Uno, H.; Kim, D. Y.; Noh, S. B.; Kim, D.; Osuka, A. *Chem. Commun.* **2005**, 3782–3784.
- (30) Sahoo, A. K.; Nakamura, Y.; Aratani, N.; Kim, K. S.; Noh, S. B.; Shinokubo, H.; Kim, D.; Osuka, A. *Org. Lett.* **2006**, *8*, 4141–4144.
- (31) Osuka, A.; Shimidzu, H. *Angew. Chem., Int. Ed.* **1997**, *36*, 135–137.
- (32) Aratani, N.; Osuka, A.; Kim, Y. H.; Jeong, D. H.; Kim, D. *Angew. Chem., Int. Ed.* **2000**, *39*, 1458–1462.
- (33) Senge, M. O.; Feng, X. D. *J. Chem. Soc., Perkin Trans. 1* **2000**, 3615–3621.
- (34) Senge, M. O.; Feng, X. D. *Tetrahedron Lett.* **1999**, *40*, 4165–4168.
- (35) Senge, M. O. *Acc. Chem. Res.* **2005**, *38*, 733–743.
- (36) Kim, P.; Ikeda, T.; Lim, J. M.; Park, J.; Lim, M.; Aratani, N.; Osuka, A.; Kim, D. *Chem. Commun.* **2011**, *47*, 4433–4435.
- (37) Scholl, R.; Mansfeld, J. *Ber. Dtsch. Chem. Ges.* **1910**, *43*, 1734–1746.
- (38) Solov'yov, K. N.; Borisevich, E. A. *Phys.-Usp.* **2005**, *48*, 231–253.
- (39) Aratani, N.; Osuka, A. *Chem. Rec.* **2003**, *3*, 225–234.
- (40) Senge, M. O.; Pintea, M.; Ryan, A. A. *Z. Naturforsch. B* **2011**, *66*, 553–558.
- (41) Kumble, R.; Palese, S.; Lin, V. S. Y.; Therien, M. J.; Hochstrasser, R. M. *J. Am. Chem. Soc.* **1998**, *120*, 11489–11498.
- (42) Rodriguez, J.; Kirmaier, C.; Holten, D. *J. Am. Chem. Soc.* **1989**, *111*, 6500–6506.
- (43) Cho, H. S.; Song, N. W.; Kim, Y. H.; Jeoung, S. C.; Hahn, S.; Kim, D.; Kim, S. K.; Yoshida, N.; Osuka, A. *J. Phys. Chem. A* **2000**, *104*, 3287–3298.
- (44) Cho, S.; Yoon, M.-C.; Kim, K. S.; Kim, P.; Kim, D. *Phys. Chem. Chem. Phys.* **2011**, *13*, 16175–16181.
- (45) Drain, C. M.; Gentemann, S.; Roberts, J. A.; Nelson, N. Y.; Medforth, C. J.; Jia, S.; Simpson, M. C.; Smith, K. M.; Fajer, J.; Shelnutt, J. A.; Holten, D. *J. Am. Chem. Soc.* **1998**, *120*, 3781–3791.
- (46) Drain, C. M.; Kirmaier, C.; Medforth, C. J.; Nurco, D. J.; Smith, K. M.; Holten, D. *J. Phys. Chem.* **1996**, *100*, 11984–11993.